PROTEINS: Structure, Function, and Genetics 20:52–67 (1994)

Structure and Dynamics of the Neutrophil Defensins NP-2, NP-5, and HNP-1: NMR Studies of Amide Hydrogen Exchange Kinetics

Jack J. Skalicky,[1] Michael E. Selsted,[2] and Arthur Pardi[1]
[1]*Department of Chemistry and Biochemistry, University of Colorado—Boulder, Boulder, Colorado 80309-0215 and*
[2]*College of Medicine, Department of Pathology, University of California—Irvine, Irvine, California 92717*

ABSTRACT **The exchange kinetics for the slowly exchanging amide hydrogens in three defensins, rabbit NP-2, rabbit NP-5, and human HNP-1, have been measured over a range of pH at 25°C using 1D and 2D NMR methods. These NHs have exchange rates 10^2 to 10^5 times slower than rates from unstructured model peptides. The observed distribution of exchange rates under these conditions can be rationalized by intramolecular hydrogen bonding of the individual NHs, solvent accessibility of the NHs, and local fluctuations in structure. The temperature dependencies of NH chemical shifts (NH temperature coefficients) were measured for the defensins and these values are consistent with the defensin structure. A comparison is made between NH exchange kinetics, NH solvent accessibility, and NH temperature coefficients of the defensins and other globular proteins. Titration of the histidine side chain in NP-2 was examined and the results are mapped to the three-dimensional structure.**

Key words: nuclear magnetic resonance, defensin, hydrogen exchange, antimicrobial peptides

INTRODUCTION

Defensins are a remarkable family of antimicrobial peptides that function in the phagocytic pathway of the mammalian immune system.[1,2] The peptides are synthesized in myeloid precursors in the bone marrow and in intestinal Paneth cells.[3–5] They are stored in the cytoplasmic granules in both cell types. The peptides have highly conserved primary structures as shown in Figure 1. Common to each of the defensins is a core of three disulfides, a glycine at residue 18, and an abundance of arginine residues. The defensins shown in Figure 1 are derived from neutrophils or macrophages, however, the peptides derived from Paneth cells share the same common structural features as myeloid defensins and probably serve as antimicrobial agents in the bowel.[3]

Purified defensins display a remarkably broad spectrum of in vitro antimicrobial activity. At micromolar concentrations many defensins can kill gram-positive and gram-negative bacteria, fungi, and enveloped viruses.[1,2,5] Certain members of the defensin family have a much broader range of specificity and potency than others. For example rabbit neutrophil peptide-2 (NP-2) is the most potent of the defensins with the broadest spectrum of activity, rabbit neutrophil peptide-5 (NP-5) is much less potent and has a limited spectrum of activity, and human neutrophil peptide-1 (HNP-1) is intermediate in its range of activity and potency. A central question in defensin biology is, "What is the relationship between the defensin structures and their quite different activities?" This question has been addressed with the recent NMR solution structures of NP-2, NP-5, and HNP-1[7,8] and a crystal structure of HNP-3.[9] An NMR solution study initially defined the three-dimensional defensin fold[6] and the same fold was subsequently identified in the X-ray study of HNP-3. Interestingly, HNP-3 crystallizes as a symmetrical dimer.[9] The solution structures of the NP-2, NP-5, and HNP-1 monomers and the crystal structure of the HNP-3 dimer are amphiphilic and these have been used to model possible mechanisms of action.[7–10] Structural information pertaining to the oligomer state may be necessary to unravel the functional mechanism of the defensins.

The kinetics of NH exchange is an important tool for characterizing the structure and dynamics of proteins.[10,11] The NH exchange behavior of proteins depends on fluctuations in their structure and the concept of structural mobility in proteins was developed in part to explain the results of NH exchange experiments.[12] NH exchange is exquisitely sensitive to structural perturbations such as those caused by ligand binding and allostery.[11] Exchange of amide hydrogens with solvent can occur via several different mechanisms. Under native conditions, the dom-

Received January 7, 1994; revision accepted May 23, 1994.
Address reprint requests to Arthur Pardi, Department of Chemistry and Biochemistry, University of Colorado—Boulder, Boulder, CO 80309-0215.

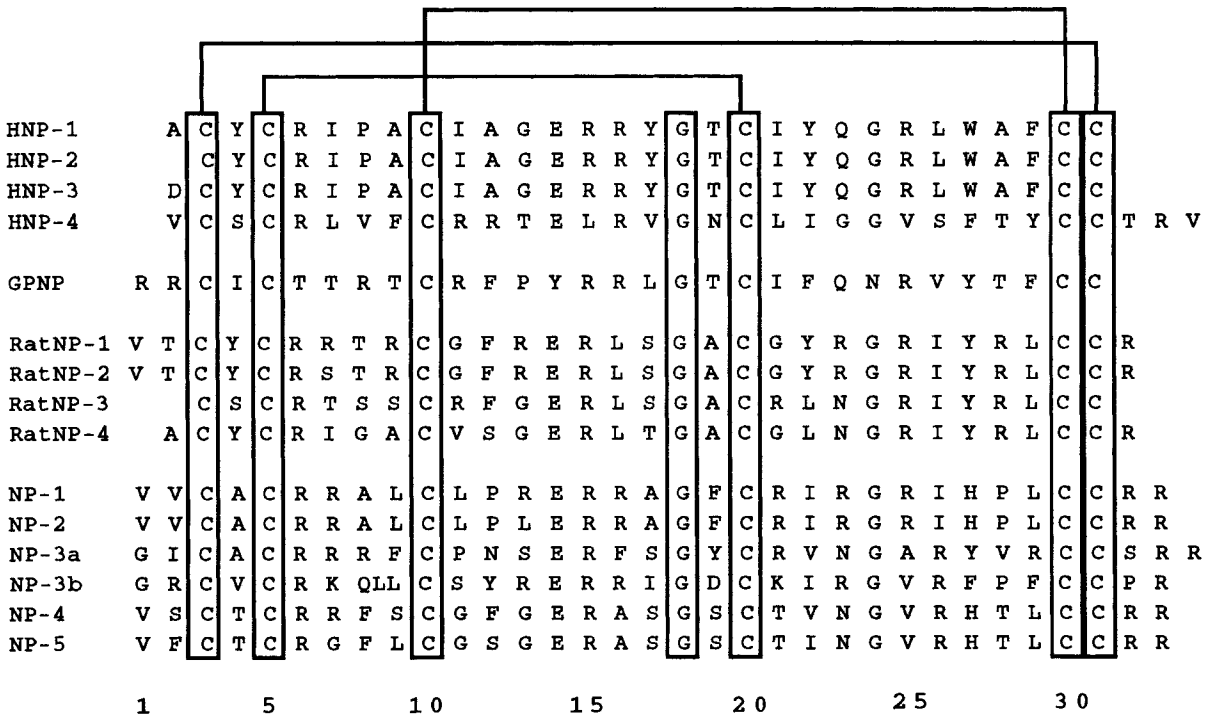

Fig. 1. The primary structures of the human, rabbit, rat, and guinea pig neutrophil-derived defensins are shown maximally aligned. The boxed regions indicate conserved residues and the lines connecting the boxes indicate disulfide bonds. Standard single letter abbreviations are used to designate the amino acids.

inant exchange mechanism for a number of the more highly protected NHs in basic pancreatic trypsin inhibitor (BPTI) is mediated by low activation energy processes;[13] these may represent local fluctuations in the structure. On the other hand, under experimental conditions that are close to the denaturation transition, exchange becomes dominated by processes of much higher activation energy such as large scale structural fluctuations.[11]

This study uses NH exchange kinetic information to characterize the defensin monomer structure, defensin dynamics, and possible intermolecular interactions. Patterns of NH exchange kinetics in the defensins NP-2, NP-5, and HNP-1 are compared and are interpreted in terms of local unfolding events.[11]

MATERIALS AND METHODS

NMR Spectroscopy

The 2D NMR spectroscopy experiments were performed on a Varian VXR-500S spectrometer. The spectra were acquired in the phase sensitive absorption mode with quadrature detection in both dimensions.[14] COSY[15,16] experiments were used to measure NH exchange for NP-2 and NP-5 and NOESY[17,18] experiments were used for HNP-1. NOESY experiments were performed on HNP-1 because the large resonance line-widths (>9 Hz) of this peptide can lead to cancellation of crosspeak and poor signal-to-noise in the correlated spectroscopy (COSY) experiments. 2D spectra were collected with the transmitter frequency centered on the residual water signal and the water signal was continuously irradiated at low power during a 1.2–1.5 s recycle delay. NP-2 and NP-5 were acquired with a 5500 Hz spectral window and HNP-1 was acquired with a 7000 Hz window. For all 2D NMR experiments, 1024 or 2048 complex points were collected during the detection period (t_2), 256–325 complex points were collected in the evolution period (t_1), and 16–64 transients were acquired for each free induction decay (FID). Each FID was then multiplied by an unshifted sine bell window function for the COSY experiments, or a 70 to 80 degree shifted sine bell function for the NOESY experiments. In the t_1 dimension the interferograms were zero filled to make a square matrix prior to Fourier transformation and window functions similar to those used in t_2 were applied in the t_1 dimension. The first point of each interferogram from a NOESY spectrum was adjusted to help eliminate t_1 ridges.[19]

One-dimensional ^{1}H-NMR spectroscopy was used for measuring some NH resonance intensities and to monitor NH exchange. 1D spectra were collected with 8192 complex points and 64 transients per FID. All NMR data were processed on a Sun 4/260 computer using the NMR processing software FELIX.

Amide Hyrogen Exchange Experiments

The defensins were isolated and purified as previously described.[20,21] NP-2 and NP-5 were prepared at concentrations of 4 and 2 mM, respectively, in 10 mM deuterated sodium succinate. HNP-1 was prepared at a concentration of 1.5 mM in 10 mM sodium phosphate. The deuterium exchange studies required complete NH occupancy prior to initiation of exchange experiments. This was accomplished by incubating the peptides in H_2O (35°C, pH 3.5–6.0) until all NDs had exchanged to NHs, as judged by the intensity of amide proton resonances in the 1D ^1H NMR spectrum. Following this procedure the peptides were lyophilized to dryness and stored at −20°C until used. Amide hydrogen exchange was initiated by dissolving the lyophilized peptide in 600 μl of 99.9% D_2O, measuring the pH, and immediately beginning data acquisition. The pH measurements were made with a standard calomel referenced microelectrode and were not corrected for isotope effects.

The COSY and NOESY NH-Hα crosspeak volumes were used to measure the fraction of NH versus ND occupancy. Crosspeaks from one side of the diagonal (ω_2 = NH, ω_1 = Hα) were measured. Since a phase-sensitive COSY crosspeak has zero integrated volume, these data were converted to absolute value mode prior to extraction of the crosspeak volume. An average of 10 volume integrals in empty regions of the 2D spectrum was used as a background value and subtracted from each crosspeak volume. The NH exchange rate constant (k_{ex}) was then determined by fitting to the expression, $A_t = A_0 \exp(-k_{ex}t)$ with a nonlinear least-squares fitting routine, where A_t is the experimental crosspeak volume, k_{ex} is the experimentally determined pseudo-first-order rate constant, and t is the elapsed time of NH→ND exchange.[22] Within the accuracy of the intensity measurements, no deviation was detected from a first-order exponential for any of the NH exchange curves.

Several NHs exchange sufficiently fast that the exchange process cannot be followed by COSY. Some of these were measured with 1D experiments. A lower limit of these rate constants can be approximated by considering the expression for NH exchange, $A_t = A_0 \exp(-k_{ex}t)$, and the fraction of exchange that has occurred before acquisition. Assuming a minimum of two datum points is required to determine a NH→ND exchange rate constant then the time required to reach the second datum point can be easily estimated from the length of a 1D or 2D experiment. The intensity ratio (A_0/A_t) for an unexchanged NH compared to a NH that has exchanged to near noise level is approximately 35/1 for several of the NHs in the defensins. Thus a lower limit of the rate constant, k_{ex}, accessible in a 120 min COSY is 0.01 min^{-1}. Likewise the lower limit for k_{ex} accessible with 1D NMR is approximately 0.08 min^{-1}.

The Dependence of NH Chemical Shift on Temperature

For measuring the temperature dependence of the NH chemical shifts of NP-2, NP-5, and HNP-1 the NMR samples were dissolved in 90% H_2O/10% D_2O and a COSY (NP-2 and NP-5) or NOESY (HNP-1) spectrum was acquired in 5°C increments from 5 to 40°C. All proton chemical shifts were measured relative to the H_2O resonance at a chemical shift of 4.75 ppm at 25°C relative to sodium 3-(trimethylsilyl)-proprionate-D_4 (TSP) and a temperature dependence of −0.01 ppm/°C over the temperature range of 5–40°C. The NH chemical shift temperature coefficients are the slopes of the NH chemical shift versus temperature plots.

Titration of NP-2

The pH dependence of certain NP-2 proton chemical shifts was recorded with a COSY spectrum at pH values from 2.5 to 8.2. Proton chemical shifts were referenced to an external standard of TSP. The pH of NP-2 was adjusted with either 0.05 M NaOH or 0.05 M HCl. Directly adding small aliquots of strong acid or base did not appear to disrupt native peptide structure as judged by the invariance of the chemical shifts for numerous C^α, methyl, and amide protons.

NH Solvent Accessible Surface Area Calculations

Solvent accessible surface areas were measured for HNP-3,[9] 20 refined NP-2 and HNP-1 structures,[8,10] five NP-5 structures,[7] oxidized tuna cytochrome c,[23] and hen egg white lysozyme.[24] Hydrogen atoms were added to the X-ray crystal structures using INSIGHTII (BIOSYM, Inc.). The water molecule was modeled by a hard sphere of 1.4 Å radius and the effective solvent accessible surface areas are reported.[25,26]

RESULTS

Identification of the Slowly Exchanging Amide Hydrogens

As seen in Table I, depending upon the pH of the exchange experiment, 30–60% of the defensin NHs have exchange rate constants smaller than 0.1 min^{-1}. The amide hydrogens that exchange with rate constants of < 0.1 min^{-1} are defined as "slowly exchanging amide hydrogens" and those amide hydrogens that exchange faster are referred to as "rapidly exchanging amide hydrogens."

NH exchange rates depend upon pH, temperature, ionic strength, and the isotope of water,[11] thus the number of slowly exchanging amide hydrogens in a peptide will vary with these solution conditions. The previously identified slowly exchanging amide hy-

TABLE I. NH→ND Exchange Rate Constants for the Defensins NP-2, NP-5, and HNP-1*

Residue	pH 2.22	pH 3.35	pH 3.97	pH 4.35	pH 4.65	pH 4.88	pH 5.82
NP-2					†		
Val-2					420 ± 71		
Ala-4	2.3 ± 0.1	4.1 ± 0.2		6.2 ± 0.2		37.0 ± 0.6	
Arg-6	1.3 ± 0.1				200 ± 8		
Leu-11	25.0 ± 0.3	3.2 ± 0.5		3.5 ± 0.4		15.1 ± 0.6	89.3 ± 2.7
Glu-14	4.3 ± 0.2	2.3 ± 0.1		3.7 ± 0.3		11.0 ± 0.5	31.0 ± 1.3
Arg-15	6.6 ± 0.4	7.0 ± 0.2		6.5 ± 0.2		25.0 ± 2.0	95.0 ± 5.6
Ala-17	9.2 ± 0.3	9.6 ± 0.3		26.0 ± 0.1			
Gly-18					290 ± 12		
Phe-19	47.0 ± 1.8						
Cys-20	1.5 ± 0.1	1.9 ± 0.1		3.8 ± 0.8		18.0 ± 1.0	55.0 ± 2.0
Ile-22	3.1 ± 0.1				230 ± 14		
Arg-25	18.3 ± 0.9				480 ± 51		
Ile-26	36.2 ± 2.3						
His-27	3.6 ± 0.2	13.0 ± 0.5		37.0 ± 0.1			
Leu-29	1.2 ± 0.1	0.6 ± 0.1		1.3 ± 0.1		3.2 ± 0.3	6.6 ± 0.2
Cys-30	1.9 ± 0.1	0.8 ± 0.1		1.4 ± 0.2		4.3 ± 0.1	8.8 ± 0.6
Cys-31	3.5 ± 0.2	4.7 ± 0.1		5.6 ± 0.7		18.0 ± 1.4	47.0 ± 2.7
Arg-32	50.7 ± 3.0						
Arg-33					680 ± 93		
NP-5							
Thr-4		2.1 ± 0.1		7.7 ± 0.3		16.0 ± 1.9	
Glu-14		8.1 ± 0.3		12.0 ± 1.2		40.0 ± 5.7	
Arg-15		6.4 ± 0.8		11.0 ± 0.6		54.0 ± 7.0	
Ser-17		7.9 ± 0.5		45.0 ± 5.2			
Cys-20		4.6 ± 0.2					
Ile-22		32.0 ± 3.5					
Val-25		10.2 ± 0.3		42.0 ± 4.7			
His-27		8.6 ± 0.6		35.0 ± 3.1			
Thr-28		67.2 ± 3.7					
Leu-29		0.38 ± 0.06		1.1 ± 0.1		4.6 ± 0.3	27.0 ± 3.0
Cys-30		0.21 ± 0.02		0.46 ± 0.1		4.8 ± 0.4	17.0 ± 3.8
Cys-31		75.0 ± 5.3					
HNP-1				†			
Tyr-4			5.6 ± 0.4	19.3 ± 2.2	26.1 ± 4.2		
Arg-6			4.4 ± 0.3		15.6 ± 2.8		
Ile-7				112 ± 7			
Ala-9				29.0 ± 2.0			
Ile-11			9.7 ± 0.4		27.0 ± 2.0		
Glu-14			8.7 ± 0.5		47.0 ± 1.3		
Arg-15			14.0 ± 0.7				
Tyr-17			1.2 ± 0.1		3.9 ± 0.2		
Gly-18				151 ± 20			
Cys-20					9.2 ± 2.0		
Ile-22			4.8 ± 0.3				
Arg-25			20.0 ± 0.2	25.0 ± 1.0			
Leu-26			15.0 ± 1.2	29.0 ± 0.8			
Trp-27			0.50 ± 0.1		0.9 ± 0.2		
Ala-28			1.1 ± 0.1		7.1 ± 0.5		
Phe-29			0.7 ± 0.3		1.0 ± 0.2		
Cys-30			0.15 ± 0.1		2.4 ± 0.6		
Cys-31			4.1 ± 0.3		20.0 ± 0.6		

*Exchange rate constants are expressed as $10^4 \times k_{ex}$ in the units of min^{-1}. The pH value is the uncorrected calomel pH meter reading in D_2O.

†One-dimensional ^{1}H-NMR was used to measure exchange rates for NP-2 at pH 4.65 and HNP-1 at pH 4.35.

drogens in the defensins include 10 in NP-2 at pH 3.5 and 30°C,[27] 9 in NP-5 at pH 3.5 and 19.8°C,[28] and 18 in HNP-1 at pH 3.5 and 30°C.[27]

Amide Hydrogen Exchange Rate Constants

The exchange rate constants for the slowly exchanging amide hydrogens in NP-2, NP-5, and

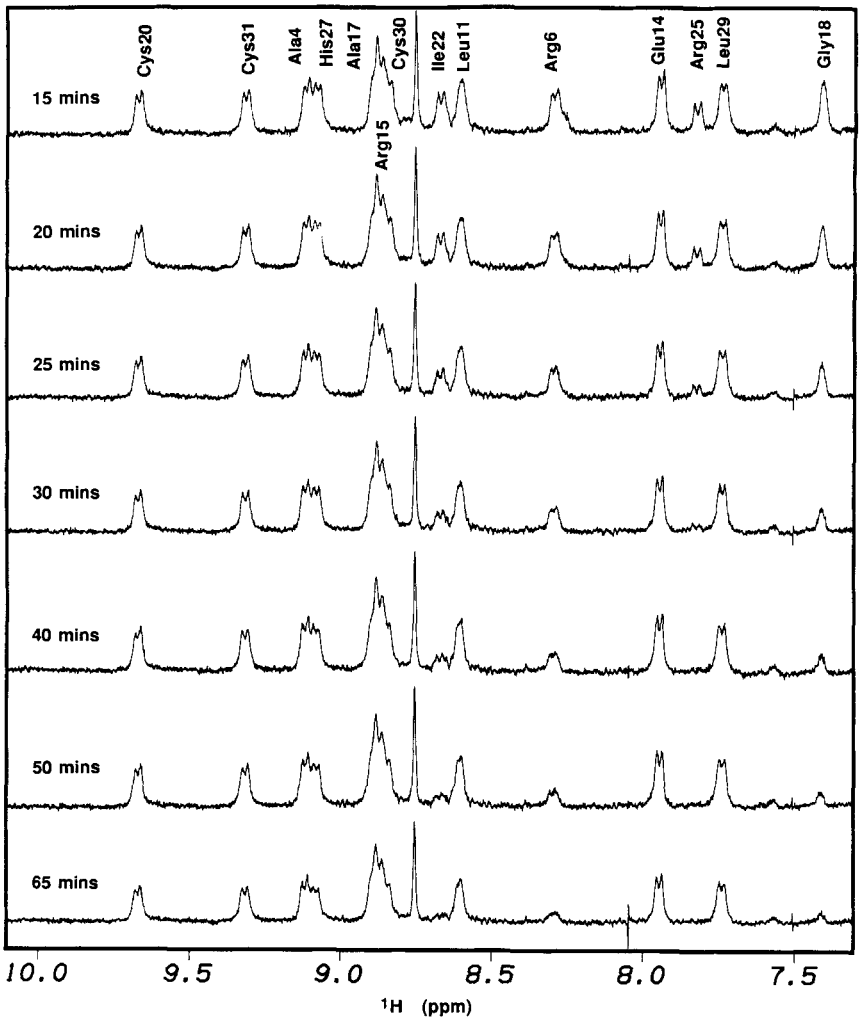

Fig. 2. 1D ^{1}H-NMR spectra for the NH region of NP-2 at 25°C, pH 4.65 showing a time course of NH→ND exchange. The time elapsed following addition of D_2O to the lyophilized peptide is indicated for each spectrum. The resonances for many of the slowly exchanging amide hydrogens are labeled in the top spectrum.

HNP-1 were measured at 25°C as a function of pH (Table I). Representative time courses of the 1D and 2D COSY experiments used to measure the exchange kinetics are shown in Figures 2 and 3, respectively. These data fit a single exponential decay curve as determined with nonlinear least-squares analysis (see Fig. 4) with rates for NH exchange given in Table I. These rates equate to NH half-lives of approximately 10^1 and 10^4 min under the conditions described. The remaining NHs exchange too quickly to be measured in these experiments.

The pH dependence of NH exchange for the nine most slowly exchanging amide hydrogens of NP-2 were examined over the pH range of 2.2 to 5.8 at 25°C and are shown in Figure 5. The dotted line in each plot of Figure 5 is the predicted curve (k_p) for NH→ND exchange given by Eq. (1) for poly-(D,L)-alanine (PDLA);[11,29,30]

$$k_p = k_{acid}[D^+] + k_{base}[OD^-] + k_{water} \quad (1)$$

where k_{acid} is 6.17×10^1 M^{-1} min^{-1}, k_{base} is 1.83×10^{10} M^{-1} min^{-1}, and direct catalysis by water (k_{water}) is 5.47×10^{-2} min^{-1} at 25°C under low salt conditions.[30] Amide hydrogen exchange (NH→ND) is catalyzed by D^+ and OD^- with direct catalysis by D_2O making a small contribution to the exchange rate near the pH where the amide hydrogen exchange rate constant is a minimum (pH_{min}).[31] Under the conditions employed here, direct catalysis by buffer bases make insignificant contributions to the amide hydrogen exchange rates.[11] The solid upper curve in each plot of Figure 5 shows the predicted curve for the indicated NP-2 residue. This was computed using Eq. (1) with modifications for the rate constants to account for sequence dependent effects.[30] The corresponding experimental NH→ND

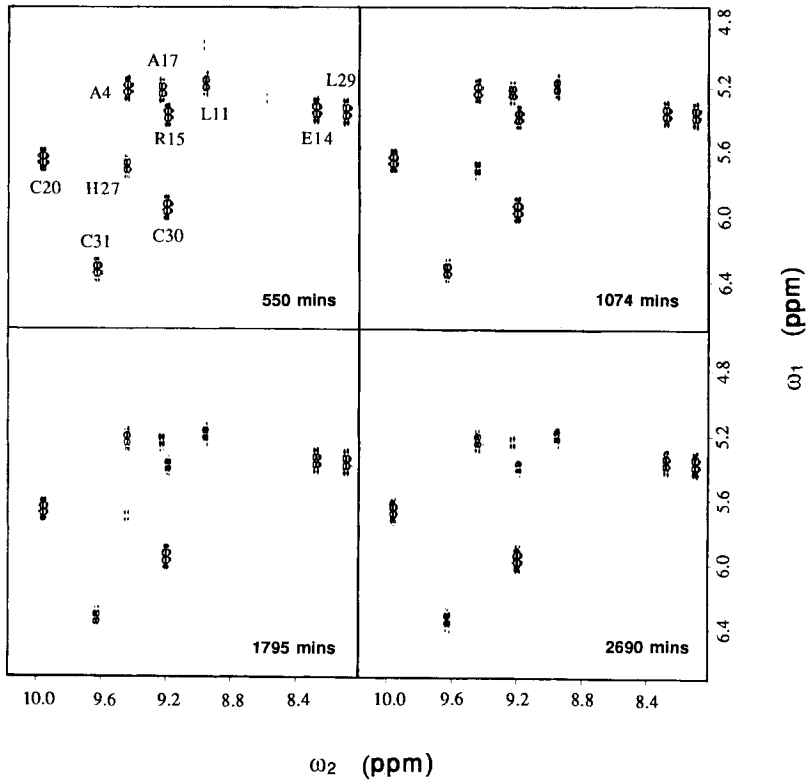

Fig. 3. The NH-Hα "fingerprint" region of a set of COSY spectra for NP-2 at 25°C, pH 3.35 showing the time course of NH→ND exchange. The time elapsed following addition of D_2O to the lyophilized peptide is calculated at the middle of the 2D experiment and indicated in the figure. Slowly exchanging amide hydrogens are labeled with standard one letter abbreviations.

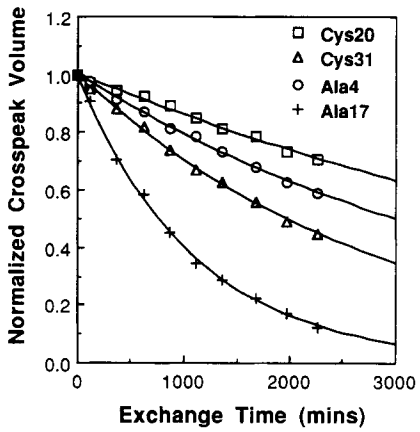

Fig. 4. Nonlinear least-squares analysis of NH exchange data showing the exponential decay of NH-Hα crosspeak volumes for four of the slowly exchanging NHs in NP-2 at pH 2.22 and 25°C.

exchange curve is shown in the lower region of each panel in Figure 5.

The most marked difference between the predicted and experimental curves is the large downward shift (from two to five orders of magnitude) in the experimental curve indicating dramatic slowing of amide hydrogen exchange. The general shape of the experimental curves is similar to predicted curves. Some of the experimental curves are less pH dependent (e.g., slopes $\neq 1$) in the base-catalyzed region such as for Leu-29, Cys-30, and Cys-31. Most of the experimental curves also have small basic shifted pH_{min} values relative to their predicted curves.

Amide Hydrogen Exchange Protection Factors

In order to compare the exchange properties of individual NHs in different peptides, protection factors were calculated for the slowly exchanging amide hydrogens in the defensins NP-2, NP-5, and HNP-1 and are shown in Figure 6. The protection factors are defined as $P = k_p/k_{ex}$, where k_{ex} is the experimental rate constant and k_p is the predicted rate constant. The k_p value was calculated for each amide hydrogen using Eq. (1) for our pH, temperature, and sequence.

Temperature Dependence of the NH Chemical Shifts

The NH temperature coefficients have been measured for the defensins from 5 to 40°C and are shown in Figure 6. In all cases the chemical shift varies

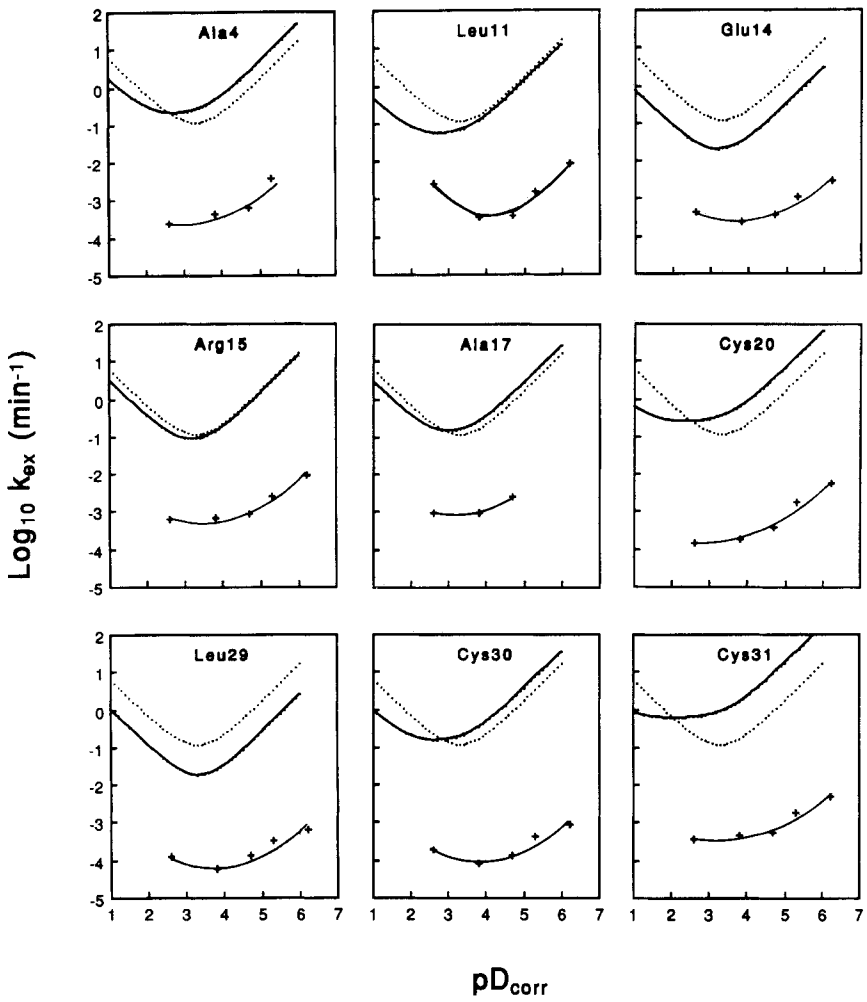

Fig. 5. NH→ND exchange curves showing the pH dependence of k_{ex} for the nine slowest exchanging amide hydrogens in NP-2. The dotted curve in each plot is the predicted exchange curve for poly-(D,L)-alanine using Eq. (1) (see text and reference 30 for additional details). The slightly shifted solid curve is the predicted NH exchange rates for the indicated residue in NP-2 at 25°C. The lower region of each plot shows the data (+) for the indicated residue, manually fit to a smooth curve. Experimental data are from Table I with the correction for the deuterium ion concentration ($pD_{corr} = pH_{read} + 0.40$) to adjust for the calomel electrode error in D_2O.[51]

linearly with temperature and nearly all the slopes are negative, ranging in value from -1.0 to -10.0×10^{-3} ppm/°C. Surprisingly, positive NH temperature coefficients are observed for Arg-32 in NP-2 and Cys-31 in NP-5. The possible significance of positive NH temperature coefficients will be discussed below. The C^{α} proton chemical shifts show no significant change over this temperature range indicating the global structures of these peptides are unchanged from 5 to 40°C.

pH Dependence of the Proton Chemical Shifts in NP-2

The effect of pH on the proton chemical shifts for a number of amide, aromatic, and C^{α} protons in NP-2 was examined and the results are shown in Figure 7 and Table II. Titration of the single histidine residue in NP-2 (His-27) was monitored by chemical shifts of the imidazole protons. The C2 and C4 protons display large chemical shift changes of 0.37 and 1.15 ppm, respectively, between the fully protonated and deprotonated states of the imidazole group. Smaller effects due to perturbations resulting from the titration of His-27 were observed for several amide protons (Leu-9, Leu-11, Cys-20, Arg-23, Gly-24, Arg-25, and Leu-29). Apparent pK_as for these protons (denoted pK_a^*) were determined by fitting the chemical shift data to Eq. (2),[32]

$$\delta(\mathrm{pH}) = \frac{\delta_{HA^+} + [\delta_A \times 10^{(\mathrm{pH} - pK_a^*)}]}{[1 + 10^{(\mathrm{pH} - pK_a^*)}]} \qquad (2)$$

where δ(pH) is the observed chemical shift (in ppm) for a particular resonance at a given pH, δ_{HA^+} is the

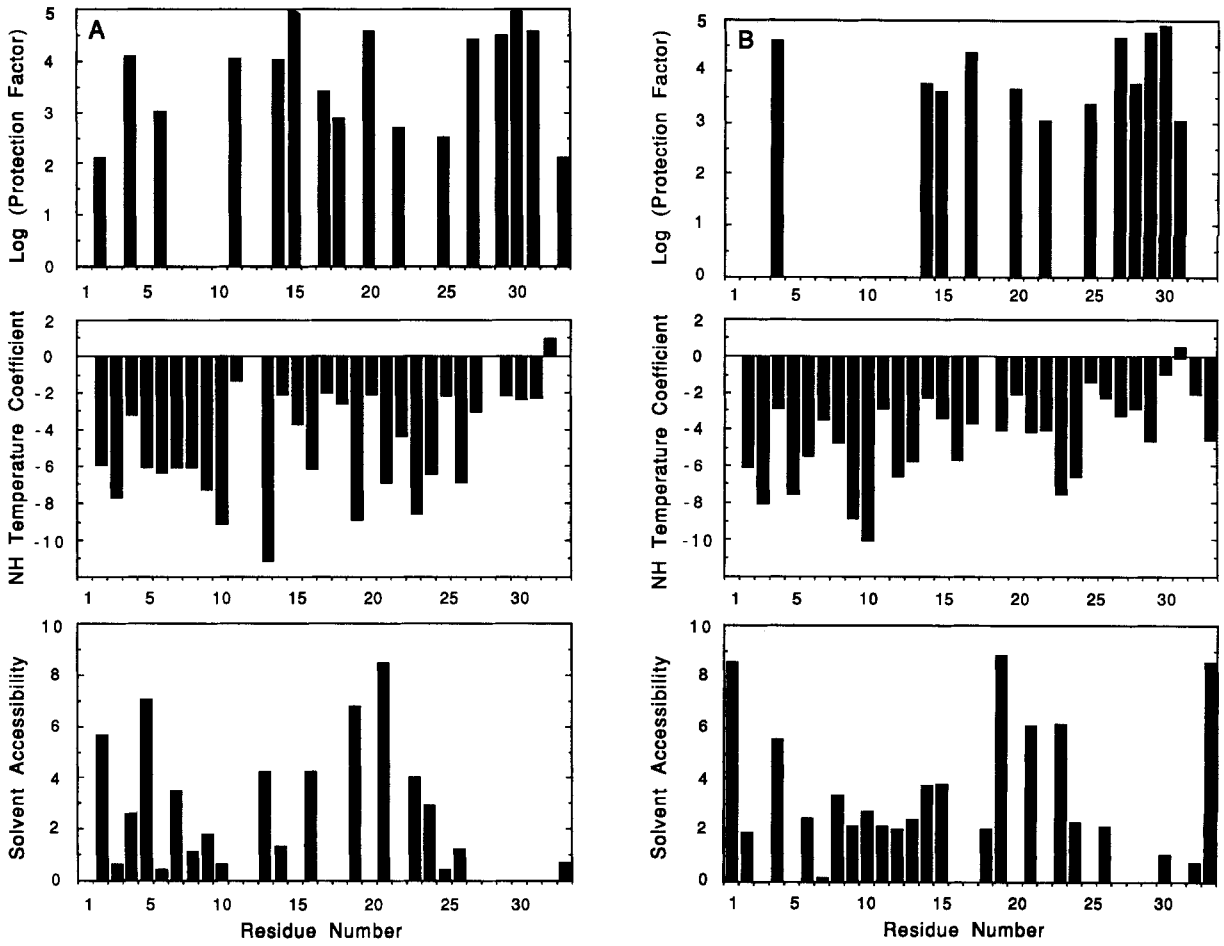

Fig. 6. The profiles of NH protection factors, NH temperature coefficients, and NH solvent accessible surface areas for the defensins are shown as a function of sequence. Top panel shows the $\log_{10}$ of the protection factors for the slowly exchanging NHs. The middle panel shows the NH temperature coefficients ($\times 10^{-3}$ ppm/°C) and the lower panel shows the NH solvent accessibility (in Å^2). **(A)** NP-2 protection factors at either pH 4.65 or 4.88 (see Table I) and NH temperature coefficients at pH 4.50. **(B)** NP-5 protection factors at either pH 4.35 or 4.88 and NH temperature coefficients at pH 4.35. **(C)** HNP-1 protection factors at either pH 4.30 or 4.60 and NH temperature coefficients at pH 4.30. (Fig. 6 continued on overleaf.)

chemical shift in the charged and protonated state, and δ_A is the chemical shift in the neutral and deprotonated state. Equation (2) assumes a single titration event is contributing to the observed proton chemical shift changes and further assumes that the peptide structure is not being perturbed over the pH range examined. The data for some protons were incomplete over the entire titration range and the apparent pK_a* for these protons was estimated visually.

Some other amide protons show pH-dependent chemical shift changes that cannot be attributed to ionization of the imidazole group. For example, the amide proton of Leu-11 shows chemical shift changes at pH values that are near the expected pK_a of the Glu-14 carboxylate. Titration of the C-terminal carboxylate was not directly observed.

DISCUSSION

The Locations of Slowly Exchanging Amide Hydrogens and Their Rates of Exchange are Tightly Coupled to Defensin Structure

As shown in Figures 5 and 6 the NH protection factors vary between 10^2 and 10^5 for the slowly exchanging NHs. This means that under our conditions the mechanism by which these amide hydrogens transiently contact the solvent, permitting exchange to occur, is not a cooperative unfolding of the structure. Rather, localized fluctuations of widely different frequencies are involved. It is thus of considerable interest to look for relationships between the distributions of exchange rates and physical features of the folded peptide.

Many previous NH exchange studies have reported correlations between slowly exchanging NHs

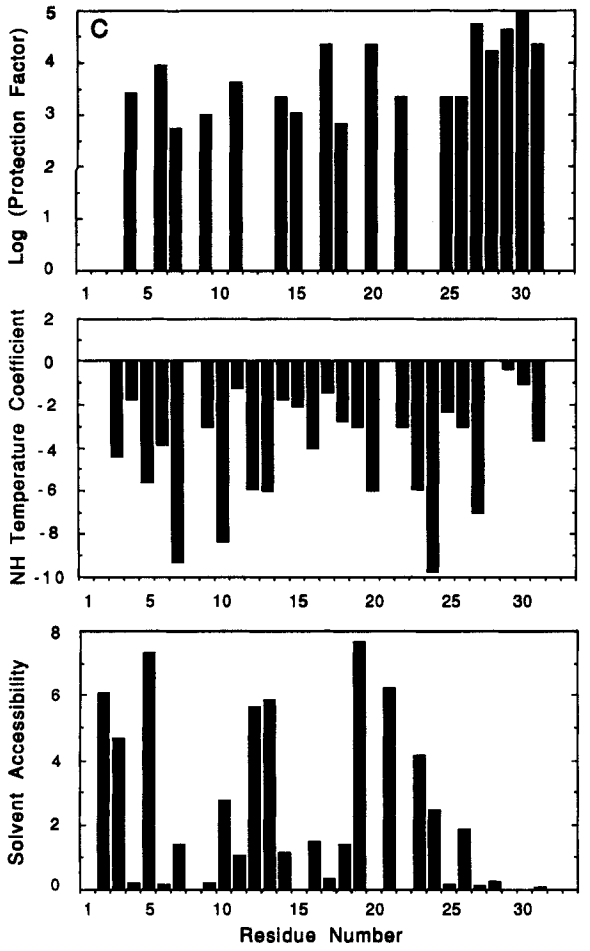

Fig. 6C.

and intramolecular hydrogen bonding.[11,33–36] In addition to intramolecular hydrogen bonds protecting amide hydrogens from exchange, intermolecular interactions can further slow the exchange of NHs that exist in intramolecular hydrogen bonds, as demonstrated in the recent study of an antigen–antibody complex.[37]

It is clear from Figure 8 that there is a good correlation, under these conditions, between slowly exchanging NHs and hydrogen bonding in the secondary structure. All of the proposed hydrogen bonding NHs in the β-sheet or β-turns of the three defensins are slowly exchanging. For example, Figure 8 shows the conserved β-hairpin structure that contains slowly exchanging NHs for residues 15, 17, 20, 22, 25, 27, 29, and 31 in all three defensins. These NHs are located on the interior of the β-hairpin. Another conserved element of secondary structure is the β-turn from residues 11–14. Slowly exchanging NHs occur at residues 11 and 14. Lastly the conserved triple stranded β-sheet region comprised of the N-terminus to residue 6 and part of the β-hairpin contain slowly exchanging NHs for residues 4 and 30. Thus the similar pattern of protection in the three defensins confirms the similar elements of secondary structure in the peptides.[7–10]

There are pronounced differences in NH exchange rates within an individual β-sheet with NH protection factors at the extremities generally smaller than at the center. For example, Figures 6 and 8 show that residues 22 and 25, located at the end of the β-hairpin, have much smaller protection factors than other slowly exchanging NHs in the hairpin. This suggests that increased fluctuations at the end of the β-hairpin contribute to the increased rate of NH exchange in this region of the peptide. Another example of this NH exchange rate pattern is observed for the NHs of the three stranded β-sheet in NP-2 (Figs. 6 and 8) where Val-2 and Arg-32 NHs have relatively small protection factors indicating mobility in this region of the β-sheet. At the opposite end of the β-sheet there is also a pattern of increasing NH protection factors from the terminus (Arg-6) to the center of the sheet (Ala-4 and Cys-30). This pattern of protection in NP-2 probably reflects fraying at the ends of the short three stranded β-sheet.

Slowly exchanging NHs in the β-sheets (see Fig. 8) are within hydrogen bonding distance (≤2.15 Å) of a backbone carbonyl oxygen in the HNP-3 X-ray structure[8] and in the respective NMR solution structures.[7,8] An apparent exception to this pattern is for Gly-18 in the defensins. This NH is >2.4 Å from a hydrogen acceptor in the X-ray crystal structure of HNP-3 and the solution structures of NP-2 and HNP-1.

Glu-14 is conserved in all of the defensins except GPNP (see Fig. 1) and its COOH is within hydrogen bonding distance (2.15 Å in one of the monomers) of the NH of residue 11 in the X-ray structure of HNP-3. This Glu-14 is also involved in a salt bridge with Arg-6 in the X-ray structure of HNP-3, but these side chains are not well defined in the defensin solution structures. However since residue 11 NH is slowly exchanging, this suggests that on the average this hydrogen bond is forming in solution. Residue 11 appears to be the only slowly exchanging NH that is hydrogen bonded to a side chain group.

As seen in Figures 6 and 8, NH exchange rates for NHs of residues near the disulfide bonds (Cys-5/Cys-20, Cys-10/Cys-30, and Cys-3/Cys-31) such as residues 4, 17, 20, 27, 29, 30, and 31 have the largest protection factors in the three defensins. This indicates that NH exchange is impeded near regions of the structure that are more constrained than others.

The locations of rapidly exchanging NHs are also conserved among the defensins. The NHs that are positioned on the exterior of the β-sheet and β-turns such as residues 3, 5, 12, 13, 16, 19, 21, 23, and 24 are rapidly exchanging in each of the defensins examined. An interesting exception is the slowly exchanging NH kinetics of residue 26 in NP-2 and HNP-1. This NH is solvent accessible in the solution structures and is not in an internal hydrogen bond.

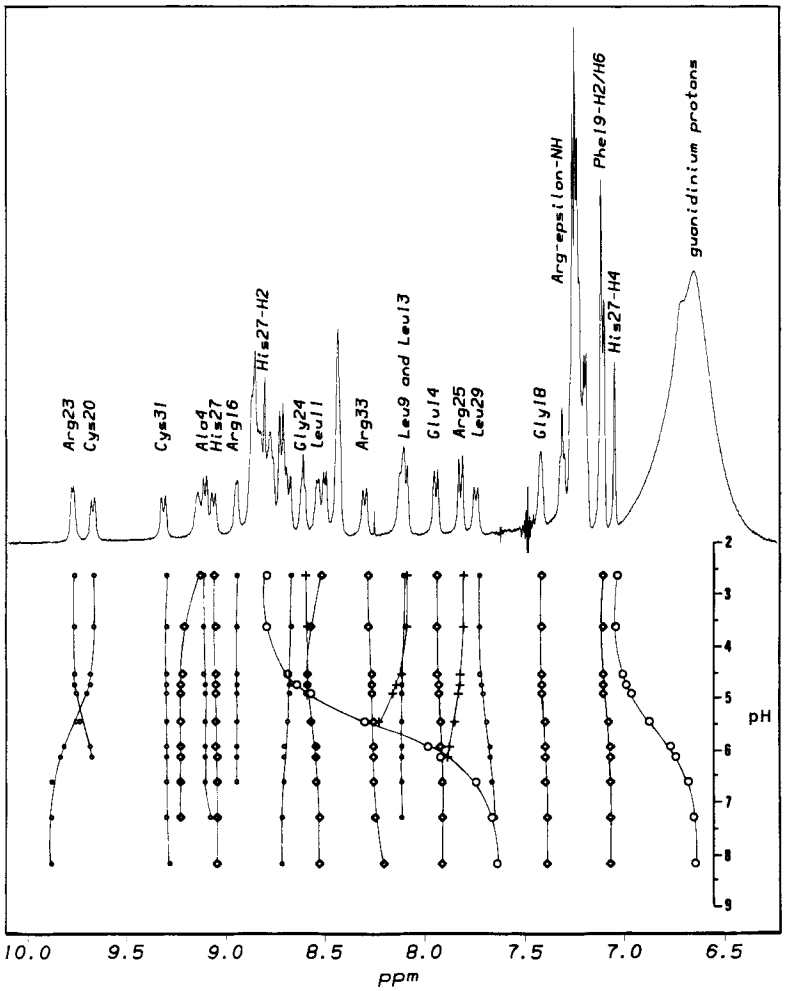

Fig. 7. The plot of pH dependence for the ^{1}H chemical shifts of amide and aromatic protons in NP-2 at 25°C. The ^{1}H NMR spectrum above the plot is for NP-2 at pH 2.60.

Perhaps specific or nonspecific intermolecular interactions are slowing this NH exchange rate.

Finally the NHs for residues 7–10 in the defensin loop region are rapidly exchanging in NP-2 and NP-5 but the NHs for residues 7 and 9 in HNP-1 are slowly exchanging (see Table I and Fig. 6). Previous studies have shown evidence that indicates HNP-1 is aggregating in solution and this may be the reason for slowed NH exchange for these residues.[27] Previous NMR studies on NP-2, NP-5, and HNP-1 also indicate this region of the peptide is dynamic,[6–10] suggesting the increased flexibility may be responsible for the rapid NH exchange kinetics observed in NP-2 and NP-5.

NH Temperature Coefficients Show Good Correlation With Amide Hydrogen Exchange Kinetics

Previous studies have shown that there is a quite good correlation of NH temperature coefficients with accessibility of amide hydrogens to solvent.[38] Thus NH temperature coefficients can be used to probe the NH microenvironment and provide additional structural information. In the defensins there is good correlation between NH temperature coefficients and NH exchange rates. The slowly exchanging NHs are on the interior of the β-sheet and β-turns and have small temperature coefficients ($< | 5.0 \times 10^{-3}$ ppm/°C |) indicating NH participation in intramolecular hydrogen bonding or NH solvent inaccessibility. In contrast, NHs on the exterior of β-sheet and β-turns generally have much larger NH temperature coefficients ($> | 5.0 \times 10^{-3}$ ppm/°C |) indicative of hydrogen bonding to waters. The similar pattern of NH temperature coefficients in the three defensins confirms their similar structure.

There are several anomalous NH temperature coefficients. The NH temperature coefficients for Arg-32 in NP-2 and Cys-31 in NP-5 are positive which is unusual. Several other NH temperature co-

TABLE II. The pH Titration Parameters of Amide and Imidazole Protons in NP-2 at 25°C

Residue	Δδ (ppm)*	pK_a*†
His-27 H4	0.37	5.5 ± 0.1
His-27 H2	1.15	5.5 ± 0.1
Cys-20 NH	−0.23	5.6 ± 0.1
Arg-25 NH	−0.09	5.7 ± 0.2
Leu-29 NH	0.06	5.4 ± 0.3
Arg-23 NH	0.09	5.7 ± 0.2
Gly-24 NH	0.07	5.5 ± 0.2
Leu-9 NH	−(0.4)	(5–6)
Leu-11 NH	−(0.2)	(2–3)

*Δδ is the proton chemical shift difference δ(low pH) − δ(high pH). A negative value indicates the proton resonance is shifting downfield as pH increases.
†These numbers are determined from fits to Eq. (2) and those in parentheses are estimated values based on visual inspection.

efficients in this region of secondary structure of the defensins are not consistent with exchange kinetics or hydrogen bonding patterns. For example, the NH temperature coefficient is larger than expected for the slowly exchanging NH of Arg-6 in NP-2. At this time there are no clear explanations for these anomalous NH temperature dependencies. Perhaps there are changes in local unfolding, dynamics, or altered interactions with nearby aromatic rings as temperature is changed.

Lastly, since the temperature coefficients are measured from 5–40°C, there is always a concern that the global structure may have changed. However, none of the Hα chemical shifts for NP-2 changed significantly (i.e., ≤ 0.01 ppm) from 5 to 40°C and the chemical shifts for the aromatic resonances of Phe-19 and His-27 and the δCH_3 resonances of Ile-22 and Ile-26 were also unchanged over this temperature range. Even at a temperature of 60°C there were no significant changes in these resonance frequencies, indicating the defensin structure is quite stable to thermal denaturation from 5 to 40°C. Thus the peptide is not globally unfolded over this temperature range and the NH temperature coefficients are probing the local structure and dynamics of the amide hydrogens.

Slowly Exchanging Amide Hydrogens Are Generally Solvent Inaccessible

Most slowly exchanging NHs in globular proteins are inaccessible to bulk solvent. For example, 64 of the 65 slowly exchanging NHs in hen egg white lysozyme[39] are not accessible to solvent. In contrast, 31 additional solvent inaccessible NHs in the hen egg white lysozyme structure are rapidly exchanging with solvent. Likewise, 43 of 44 slowly exchanging NHs in oxidized horse cytochrome *c*[40,41] are not accessible to solvent in the homologous oxidized tuna cytochrome *c* crystal structure[23] and numerous NHs that are not accessible to solvent are rapidly exchanging. Thus almost all of the slowly exchanging NHs in these proteins are solvent inaccessible. Furthermore the presence of rapidly exchanging NHs that are solvent inaccessible in the static structure indicates that dynamics of the molecule may be responsible for their exchange rates.

NH exchange kinetics in NP-2, NP-5, and HNP-1 show a good relationship with NH solvent accessibility as shown in Figure 6. For example, 26 of the 31 NHs in NP-2 are slowly exchanging when they are solvent inaccessible and are rapidly exchanging when they are solvent accessible. An exception to this rule occurs for the NHs of Val-2, Arg-6, and Arg-32 in NP-2. These solvent inaccessible NHs reside near the termini of the short triple stranded β-sheet of the structure that may be transiently exposed to solvent upon fraying. Thus as was observed in hen egg white lysozyme, cytochrome *c*, and the defensins dynamics will play a key role in determining the exchange kinetics for amide hydrogens.

Comparison of these proteins clearly indicates that NH accessibility to solvent is an important factor for slowing NH exchange kinetics, although other factors also contribute to exchange. Indeed, conclusions about solvent accessibility derived from static structures cannot adequately explain all NH exchange kinetics, and in many cases protein dynamics will need to be considered. In conclusion, slowly exchanging NHs in the defensins and other small globular proteins are generally solvent inaccessible.

pH Dependence of Amide Hydrogen Exchange

The pH dependence of the amide hydrogen exchange rates for the nine most slowly exchanging NHs in NP-2 are compared to the predicted NH exchange rates and are shown in Figure 5. The experimental NH exchange rate curves are substantially shifted downward, indicating the slower NH exchange rates, and have shapes similar to the predicted curves. NH exchange curves for Leu-29, Cys-30, and Cys-31 do not show the expected first-order dependence on pH in the base-catalyzed regime. This effect could arise from a pH induced change in the local electrostatics,[42] a change in local or global structure, or a change in dynamics. For the NHs of these residues the protection factors are somewhat larger at conditions that approach neutrality (pH≥ 5) and are smaller under more acid conditions (pH 3.0) suggesting the peptide structure may be more stable at the higher pH. This effect could also be explained assuming a shift in an equilibrium between locally unfolded states and the native conformation. A shift in equilibrium that favors the population of unfolded states at the lower pH would result in an enhanced rate of NH exchange. Similar curves for pH-dependent NH exchange kinetics have been observed for internal amide hydrogens in

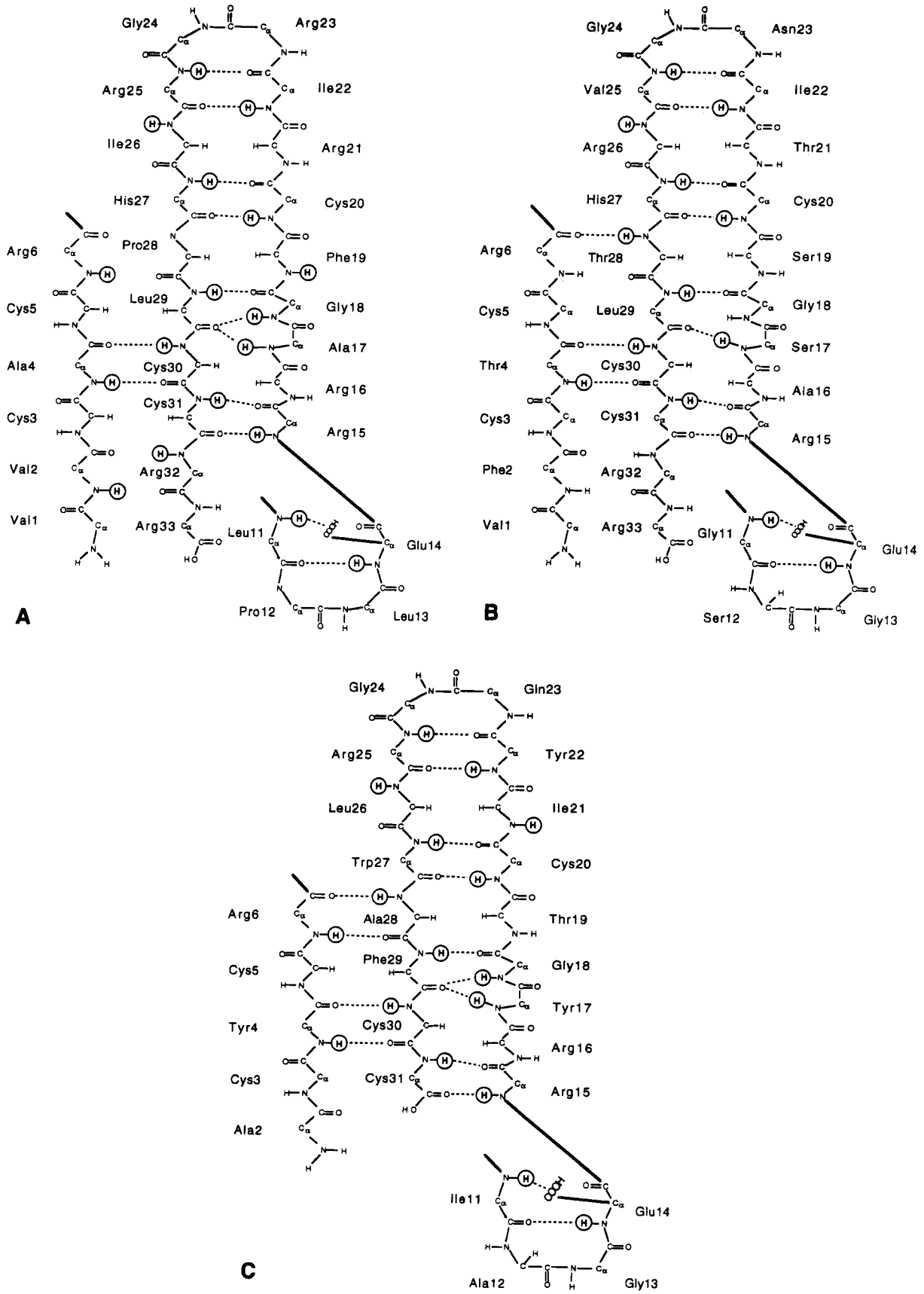

Fig. 8. A schematic diagram showing the conserved elements of secondary structure in the defensins **(A)** NP-2, **(B)** NP-5, and **(C)** HNP-1. Proposed hydrogen bonds are indicated with dashed lines and the slowly exchanging amide hydrogens are circled. The loop region in these defensins, from residues 7–10, and the disulfide bonds are not shown. NHs from residues 7 and 9 are slowly exchanging in HNP-1 but are not shown in this figure.

BPTI,[43] hen egg white lysozyme,[42] and the S-protein of ribonuclease S.[44]

The pH_{min} values are between 3 and 4 for the amide hydrogens in NP-2 and they show a small basic shift compared to the predicted curves[11,29] from model peptides. A $pH_{min} > 3$ is normally observed for NHs in globular proteins.[11] This is still somewhat unexpected since NP-2 is a positively charged peptide (+8) over a wide range of pH and a previous study on a positively charged polypeptide, poly-(D,L)-lysine, showed an acid shift in pH_{min}.[45] The acid shift for poly-(D,L)-lysine was explained by Manning counterion condensation theory for polyelectrolytes,[46] where the positive electrostatic potential at the protein surface will condense anions (such as OH^-) on the surface and effectively raise the local pH.[45] The basic shifts observed in NP-2 are opposite of those for poly-(D,L)-lysine indicating that NP-2 is certainly not behaving the same as poly-(D,L)-lysine. Furthermore, it is not that surprising that empirical rules for predicting pH_{min} cannot explain these data since these rules[29,30] account only for the inductive and steric effects of nearest neighbor residues in the peptide and do not account for secondary or tertiary structural effects or pH-induced effects on the peptide structure. Thus the small basic shifts of the pH_{min} in the amide hydrogen exchange properties of NP-2 are likely due to local structure effects similar to that observed in other small globular proteins.[11]

The NH of Leu-11 in NP-2 has the most basic shifted pH_{min} and shows the largest curvature of its pH-dependent exchange profile in the acid-catalyzed regime of NH exchange (Fig. 5). As discussed above, this NH is within hydrogen bonding distance of the carboxylate O^{ε} atom of Glu-14 in the X-ray structure of HNP-3.[9] Thus the unique pH dependence (from pH 2.2 to 5.8) of Leu-11 NH exchange rates may reflect titration of the Glu-14 carboxylate group in NP-2. The X-ray structure of HNP-3 shows that Glu-14 is involved in a salt bridge with Arg-6 and the hydrogen exchange data here indicate that the Glu-14 carboxylate also forms an internal hydrogen bond in each of the defensins. The hydrogen bond may stabilize the loop and β-turn in this region of the peptide. Supporting this conclusion is an observation that the NH of Leu-11 of HNP-1 shows a large chemical shift change (~0.8 ppm) over the pH range of 3.5–4.5 suggesting spatial proximity of the Leu-11 to a titrating carboxylate group.

Amide Hydrogen Exchange Evidence for a Defensin Dimer

The most convincing data available in support of a defensin dimer is the observation that HNP-3 crystallizes as a symmetrical dimer stabilized with four intermolecular hydrogen bonds, bridging water molecules, and several van der Waals contacts.[9] The HNP-3 dimer is unusually stable under the strongly denaturing conditions of 9 M urea or acidic pH (pH 2.3) (M.E. Selsted, unpublished results). Equilibrium sedimentation studies[8] also indicate that HNP-3 migrates at a molecular weight consistent with a dimer. Thus a defensin dimer may be the functional species and knowledge of the defensin aggregation state may be quite important for understanding the mechanism of action of these peptides. The locations of slowly exchanging amide hydrogens in NP-2 and HNP-1 suggest intermolecular interactions. For example, a previous NMR study of HNP-1 showed the NH of residue 21 is slowly exchanging.[27] Here Phe-19 NH of NP-2 was identified as slowly exchanging at pH 2.22 (Table I) even though the protection factor was quite small. The small protection factors for NHs at the proposed dimer interface (residue 19 and 21) are consistent with rapid exchange between the monomer and dimer.

pH Studies: NP-2 Structure and Stability

The pH dependence of the proton chemical shifts in NP-2 revealed interesting structural information. The imidazole group of His-27 titrates with a pK_a of 5.5 (Table II). In contrast, the pK_a of the imidazole in the tripeptide Gly-His-Gly is 6.8.[47] This difference may be a result of local structure that stabilizes the deprotonated form of the imidazole or destabilizes the protonated form. The former may be accomplished by packing of the deprotonated imidazole against a nearby hydrophobic group, such as Pro-28. This is supported by the NOE crosspeaks between proline protons and histidine protons in the solution structures of NP-2.[27] The latter is possible if a hydrophobic moiety was close to a charged imidazole group or the positively charged protonated form of imidazole could be destabilized by a nearby positively charged residue in NP-2. For example, the side chains of Arg-25 and Arg-7 are candidates for such a destabilizing charge–charge interaction, but direct evidence for these interactions is not possible since the conformation of these side chains is not determined in the NMR solution structures of NP-2.[8,27]

As shown in Figure 7 several NHs exhibit pH titration effects, and the apparent pK_a* values for most of the effected NHs are similar to the pK_a of the imidazole. These results suggest that the affected NHs are in promixity of the imidazole or that a structural change accompanies ionization of the imidazole that modifies the NH microenvironment. The invariant C^{α} proton chemical shifts, however, indicate that the peptide conformation is not significantly changing over this pH range, although small local structural changes cannot be ruled out from these data.

Figure 9 shows the NHs of Cys-20, Arg-23, Gly-24, Arg-25, and Leu-29 that are affected by the pH titration of His-27 and the proximity of these atoms to the imidazole group in the NMR solution structure

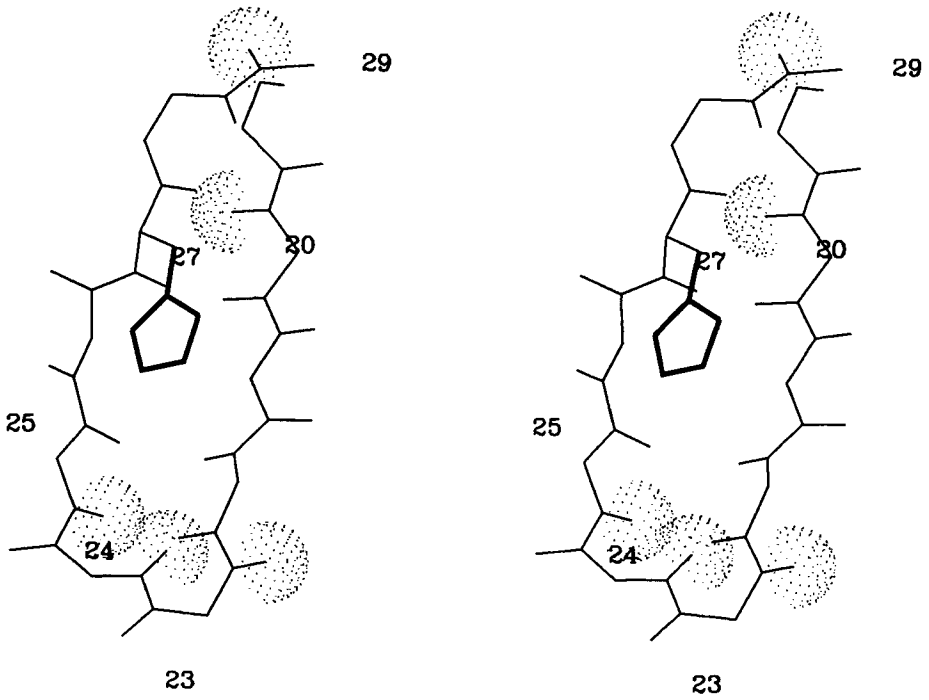

Fig. 9. Stereoview of the NP-2 β-hairpin structure.[8,10] The amide hydrogens affected by the pH titration are shown with their van der Waals surfaces and the imidazole group of His-27 is shown in bold. Residue numbers are given for the NHs that are affected by pH titration of the imidazole group.

of NP-2. Three of the affected amide protons, Arg-23, Gly-24, and Arg-25, are positioned near the terminus of the β-hairpin and each is approximately 5 Å from the center of the imidazole ring. The amide protons of Cys-20 and Leu-29 are approximately 5 and 7 Å, respectively, from the imidazole. Interestingly, both upfield and downfield amide proton chemical shifts are observed (Table II) indicating that the imidazole can have opposing chemical shift effects on nearby protons. The change in the imidazole ionization state will clearly affect the local electrostatic environment and therefore the chemical shifts of nearby NHs.

The pH titration effect on Leu-9 NH is more difficult to rationalize based on proximity to the imidazole since this NH is approximately 10 Å from the imidazole group and the imidazole group cannot be moved closer to Leu-9 in an obvious manner. A local structural change, induced by the ionization state of the imidazole, may be responsible for this "long-range" effect. In conclusion, the pH titration data presented here are generally consistent with the NP-2 structure and indicate that the imidazole group of His-27 is likely constrained to a single conformation.

CONCLUSION

These NMR data show a clear relationship between slowed amide hydrogen exchange kinetics and NH hydrogen bonding in the defensins NP-2, NP-5, and HNP-1. The similarity in positions of slowly exchanging amide hydrogens in the peptides supports the similarity in overall structure and dynamics of the defensins. Slowly exchanging amide hydrogens ($k_{ex} < 0.1$ min^{-1}) are usually solvent inaccessible, however, quantitative correlations of NH solvent accessibility and NH exchange rates require knowledge of both the structure and dynamics of the protein. There is a good correlation between NH temperature coefficients, which probe solvent accessibility,[38] and amide hydrogen exchange kinetics. The amide hydrogen exchange data are consistent with previously proposed functional models of the defensins,[6–10] however, they do not allow us to distinguish between them. Lastly, it is apparent that amide hydrogen exchange cannot be strictly correlated to a single physical parameter, and a complete understanding of exchange may require the analysis of contributions from hydrogen bonding,[11] solvent accessibility,[48] electrostatics,[42] local stability,[49] depth of amide hydrogen from solvent surface,[49,50] and the local and global dynamics.[10,11]

ACKNOWLEDGMENTS

We thank Drs. S.W. Englander, Ping F. Yip, and Lawrence P. McIntosh for helpful discussions. This work was supported in part by funds from NIH AI 22931 and AI 31696 to M.E.S. and NIH AI 27026

and a NIH Research Career Development Award (AI01051) to A.P. The 500 MHz spectrometer was purchased with partial support from NIH grant RR03283.

REFERENCES

1. Lehrer, R.I., Ganz, T., Selsted, M.E. Defensins: Endogenous antibiotic peptides of animal cells. Cell 64:229–230, 1991.
2. Ganz, T., Oren, A., Lehrer, R.I. Defensins: microbicidal and cytotoxic peptides of mammalian host defense cells. Med. Microbiol. Immunol. (Berl) 181:99–105, 1992.
3. Ouellette, A.J., Greco, R.M., James, M., Frederick, D., Naftilan, J., Fallon, J.T. Developmental regulation of cryptdin, a cortocostatin/defensin precursor mRNA in mouse small intestinal crypt epithelium. J. Cell Biol. 108: 1687–1695, 1989.
4. Selsted, M.E., Miller, S.I., Henschen, A.H., Ouellette, A.J. Enteric defensins: Antibiotic peptide components of intestinal host defense. J. Cell Biol. 118:929–936, 1992.
5. Jones, D.E., Bevins, C.L. Paneth cells of the human small intestine express an antimicrobial peptide gene. J. Biol. Chem. 267:23216–23225, 1992.
6. Ganz, T., Selsted, M.E., Lehrer, R.I. Defensins. Eur. J. Haematol. 44:1–8, 1990.
7. Pardi, A., Hare, D.R., Selsted, M.E., Morrison, R.D., Bassolino, D.A., Bach, A.2. Solution structures of the rabbit neutrophil defensin NP-5. J. Mol. Biol. 201:625–636, 1988.
8. Pardi, A., Zhang, X., Selsted, M.E., Skalicky, J.J., Yip, P.F. NMR studies of defensin antimicrobial peptides. 2. Three-dimensional structures of rabbit NP-2 and human HNP-1. Biochemistry 31:11357–11364, 1992.
9. Hill, C.P., Yee, J., Selsted, M.E., Eisenberg, D. Crystal structure of defensin HNP-3, an amphiphilic dimer: Mechanisms of membrane permeabilization. Science 251:1481–1485, 1991.
10. Skalicky, J.J. Structure-function studies of an antimicrobial family of peptides, the defensins, and a calcium channel antagonist, ω-conotoxin GVIA: NMR spectroscopy and molecular dynamics. Ph.D. Thesis University of Colorado, 1993.
11. Englander, S.W., Kallenbach, N.R. Hydrogen-exchange and structural dynamics of proteins and nucleic-acids. Q. Rev. Biophys. 16:521–655, 1983.
12. Linderstrom-Lang, K.U., Schellman, J.A. Protein structure and enzymatic activity. In: "The Enzymes." New York: Academic Press, 1959.
13. Woodward, C.K., Hilton, B.D. Hydrogen isotope exchange kinetics of single protons in bovine pancreatic trypsin-inhibitor. Biophys. J. 32:561–575, 1980.
14. States, D.J., Haberkorn, R.A., Ruben, D.J. A 2-dimensional nuclear overhauser experiment with pure absorption phase in 4 quadrants. J. Magn. Reson. 48:286–292, 1982.
15. Aue, W.P., Bartholdi, E., Ernst, R.R. 2-Dimensional spectroscopy—Application to nuclear magnetic resonance. J. Chem. Phys. 64:2229–2246, 1976.
16. Nagayama, K., Kumar, A., Wüthrich, K., Ernst, R.R. Experimental techniques of two-dimensional correlated spectroscopy. J. Magn. Reson. 40:321–334, 1980.
17. Macura, S., Ernst, R.R. Elucidation of cross relaxation in liquids by 2-dimensional nmr-spectroscopy. Mol. Phys. 41: 95–117, 1980.
18. Kumar, A., Ernst, R.R., Wüthrich, K. A Two-dimensional nuclear overhauser enhancement (2D NOE) experiment for the elucidation of complete proton-proton cross-relaxation networks in biological macromolecules. Biochem. Biophys. Res. Commun. 95:1–6, 1980.
19. Otting, G., Widmer, H., Wagner, G., Wüthrich, K. Origin of t_1 and t_2 ridges in 2D NMR spectra and procedures for suppression. J. Magn. Reson. 66:187–193, 1986.
20. Selsted, M.E., Szklarek, D., Lehrer, R.I. Purification and antibacterial activity of antimicrobial peptides of rabbit granulocytes. Infect. Immun. 45:150–154, 1984.
21. Selsted, M.E., Harwig, S.S., Ganz, T., Schilling, J.W., Lehrer, R.I. Primary structures of three human neutrophil defensins. J. Clin. Invest. 76:1436–1439, 1985.
22. Barksdale, A.D., Rosenberg, A. Acquisition and interpretation of hydrogen exchange data from peptides, polymers, and proteins. Methods Biochem. Anal. 28:1–113, 1982.
23. Takano, T., Dickerson, R.E. Conformation change of cytochrome c. II. Ferricytochrome c refinement at 1.8 Ångstöms and comparison with the ferrocytochrome c structure. Protein databank file is pdb3cyt.ent. J. Mol. Biol. 153:95–115, 1981.
24. Diamond, R. Real space refinement of the structure of hen egg-white lysozyme. Protein databank file is pdb1lyz.ent. J. Mol. Biol. 82:371–391, 1974.
25. Lee, B., Richards, F.M. The interpretation of protein structures: Estimation of static accessibility. J. Mol. Biol. 55: 379–400, 1971.
26. Richards, F.M. Areas, volumes, packing and protein structure. Annu. Rev. Biophys. Bioeng. 6:151–176, 1977.
27. Zhang, X.L. Solution structures of antimicrobial peptides determined by nuclear magnetic resonance spectroscopy and distance geometry techniques. Ph.D. Thesis Rutgers University, 1989.
28. Bach, A.C., Selsted, M.E., Pardi, A. Two-dimensional NMR studies of the antimicrobial peptide NP-5. Biochemistry 26:4389–4397, 1987.
29. Molday, R.S., Englander, S.W., Kallen, R.G. Primary structure effects on peptide group hydrogen exchange. Biochemistry 11:150–158, 1972.
30. Bai, Y.W., Milne, J.S., Mayne, L., Englander, S.W. Primary structure effects on peptide group hydrogen exchange. Proteins 17:75–86, 1993.
31. Gregory, R.B., Knox, D.G., Percy, A.J., Rosenberg, A. Thermodynamics of structural fluctuations in lysozyme as revealed by hydrogen-exchange kinetics. Biochemistry 21: 6523–6530, 1982.
32. Wüthrich, K., Wagner, G. Nuclear magnetic resonance of labile protons in the basic pancreatic trypsin inhibitor. J. Mol. Biol. 130:1–18, 1979.
33. Henry, G.D., Weiner, J.H., Sykes, B.D. Backbone dynamics of a model membrane-protein—measurement of individual amide hydrogen-exchange rates in detergent-solubilized m13 coat protein using c-13 nmr hydrogen-deuterium isotope shifts. Biochemistry 26:3626–3634, 1987.
34. Linse, S., Teleman, O., Drakenberg, T. Ca^{2+} binding to calbindin-d9k strongly affects backbone dynamics—measurements of exchange-rates of individual amide protons using ^{1}H-NMR. Biochemistry 29:5925–5934, 1990.
35. Perrin, C.L., Dwyer, T.J., Rebek, J., Duff, R.J. Exchange of amide protons—effect of intramolecular hydrogen-bonding. J. Am. Chem. Soc. 112:3122–3125, 1990.
36. Kossiakoff, A.A., Ultsch, M., White, S., Eigenbrot, C. Neutron structure of subtilisin BPN': effects of chemical environment on hydrogen-bonding geometries and the pattern of hydrogen-deuterium exchange in secondary structure elements. Biochemistry 30:1211–1221, 1991.
37. Paterson, Y., Englander, S.W., Roder, H. An antibody binding site on cytochrome c defined by hydrogen exchange and two-dimensional NMR. Science 249:755–759, 1990.
38. Jimenez, M.A., Nieto, J.L., Rico, M., Santoro, J., Herranz, J., Bermejo, F.J. A study of the NH NMR signals of Gly-Gly-x-Ala tetrapeptides in water at low temperature. J. Mol. Structure 143:435–438, 1986.
39. Redfield, C., Dobson, C.M. Sequential 1H NMR assignments and secondary structure of hen egg white lysozyme in solution. Biochemistry 27:122–136, 1988.
40. Wand, A.J., Roder, H., Englander, S.W. Two-dimensional ^{1}H NMR studies of cytochrome c: Hydrogen exchange in the N-terminal helix. 25:1107–1114, 1986.
41. Jeng, M.F., Englander, S.W., Elove, G.A., Wand, A.J., Roder, H. Structural description of acid-denatured cytochrome c by hydrogen exchange and 2D NMR. Biochemistry 29:10433–10437, 1990.
42. Delepierre, M., Dobson, C.M., Karplus, M., Poulsen, F.M., States, D.J., Wedin, R.E. Electrostatic effects and hydrogen exchange behaviour in proteins. The pH dependence of exchange rates in lysozyme. J. Mol. Biol. 197:111–130, 1987.
43. Richarz, R., Sehr, P., Wagner, G., Wüthrich, K. Kinetics of the exchange of individual amide protons in the basic pancreatic trypsin inhibitor. J. Mol. Biol. 130:19–30, 1979.
44. Rosa, J.J., Richards, F.M. An experimental procedure for

increasing the structural resolution of chemical hydrogen-exchange measurements on proteins: Application to ribonuclease S peptide. J. Mol. Biol. 133:399–416, 1979.
45. Kim, P.S., Baldwin, R.L. Influence of charge on the rate of amide proton-exchange. Biochemistry 21:1–5, 1982.
46. Manning, G.S. The molecular theory of polyelectrolyte solutions with applications to the electrostatic properties of polynucleotides. Q. Rev. Biophys. 11:179–246, 1978.
47. Markley, J.L. Observation of histidine residues in proteins by means of nuclear magnetic resonance spectroscopy. Acc. Chem. Res. 8:70–80, 1975.
48. Wagner, G. Characterization of the distribution of internal motions in the basic pancreatic trypsin inhibitor using a large number of internal NMR probes. Q. Rev. Biophys. 16:1–57, 1983.
49. Rashin, A.A. Correlation between calculated local stability and hydrogen exchange rates in proteins. J. Mol. Biol. 198:339–349, 1987.
50. Constantine, K.L., Freidrichs, M.S., Goldfarb, V., Jeffrey, P.D., Sheriff, S., Mueller, L. Characterization of the backbone dynamics of an anti-digoxin antibody V_L domain by inverse detected ^{1}H-^{15}N NMR: Comparisons with x-ray data for Fab. Proteins 15:290–311, 1993.
51. Glasoe, P.F., Long, F.A. Use of glass electrodes to measure acidities in deuterium oxide. J. Phys. Chem. 64:188–193, 1960.